Preparation of Metal-Incorporated SAPO-34 catalysts and their Catalytic Performance in Selective Catalytic Reduction of Nitric Oxide

*Dapeng Wang[a], Yi Yang[b], Chengwen Song[b]**

a Dalian Maritime University, Navigation College, 1 Linghai Road, Dalian 116026, China
b Dalian Maritime University, College of Environmental Science and Engineering, 1 Linghai Road, Dalian 116026, China

Metal-incorporated SAPO-34 catalysts were prepared by one-step hydrothermal method. Effects of various parameters including the types of metal ions, Cu^{2+} sources, structure directing agents (SDAs), hydrothermal temperature and time on catalyst activity of the metal-incorporated SAPO-34 catalysts were investigated. Three types of metal-incorporated SAPO-34 catalysts (Cu/SAPO-34, Fe/SAPO-34 and Mn/SAPO-34) were successfully obtained. Compared with Fe/SAPO-34 and Mn/SAPO-34 catalysts, Cu/SAPO-34 catalyst revealed complete cubic-like microstructure, wide active temperature window and high conversion rate in selective catalytic reduction (SCR) of nitric oxide. After defined Cu^{2+} was the favorable active site of SAPO-34 catalyst, the effects of four Cu^{2+} sources on SCR performance were further investigated, and found Cu^{2+} sources did not produce significant influence on nitric oxide conversion rates. SDAs determined the formation of Cu/SAPO-34 catalyst, and the Cu/SAPO-34 catalyst adopting tetraethylenepentamine (TEPA) as SDA could maintain higher crystal integrity and active sites, which were in favor of the SCR reaction. Moreover, hydrothermal temperature and time had great influences on the formation of Cu/SAPO-34 catalyst. When the hydrothermal temperature was higher than 150 °C and the hydrothermal time was longer than 3 days, the Cu/SAPO-34 catalyst with a cubic-like structure and high catalyst activity could be obtained.

Keywords: *Selective catalytic reduction, Cu/SAPO-34, catalyst activity, nitric oxide.*

1. Introduction

Nitrogen oxides (NO_x), as one of the major atmospheric pollutants, are mainly generated in the combustion of fossil fuels and biofuels, which have given rise to serious environmental problems including greenhouse effect, ozone depletion, acid rain[1-5]. At present, selective catalytic reduction (SCR) has been applied as one of the most effective methods on NO_x removal in flue gas[6-8]. Compared with noble metal or oxides catalysts, SAPO-34 catalysts demonstrate high NO_x conversion efficient and arise widespread concern. However, SAPO-34 catalysts are extremely sensitive to humid environment, which easily causes serious structure deterioration because of the irreversible hydrolysis of bridge hydroxyl group[9-11].

Recently, great efforts have been carried out to improve the SCR activity by doping transition metals into SAPO-34 catalysts. According to previous reports, Fe-incorporated catalyst exhibited enhanced NO_x conversion at high temperature[12-15]. Mn-incorporated catalyst was also developed to improve low-temperature SCR activity[16-18]. Besides, introducing Cu^{2+} into SAPO-34 catalysts could increase theirs low-temperature hydrothermal stability owing to the enhanced stabilization of negative Si-O-Al connections[19]. Among the metal-incorporated catalysts, Cu-incorporated catalysts demonstrated excellent potential owing to their low price, high catalytic activity, wide temperature range[20,21].

Currently, Cu/SAPO-34 catalysts could be fabricated by three methods: impregnation, ion-exchange, and one-pot methods. Generally, the distribution of copper species is closely related to the synthesis method[22,23]. Specially, ion-exchange and one-pot methods were more favorable due to more active sites generation and less structure damages[13,24,25]. Wang et al.[26] adopted ion-exchange method to fabricate Cu/SAPO-34 catalysts, which demonstrated Cu species existing as isolated ions were active sites for the SCR reaction. Fickel et al.[20] also utilized ion-exchange method to fabricate Cu/SAPO-34 catalysts. Their work demonstrated Cu/SAPO-34 catalysts with high SCR activity could be achieved even after steaming. Meanwhile, Liu et al.[27] reported their work on Cu/SAPO-34 catalysts obtained by ion-exchange method. They believed that the migration of surface CuO clusters into the ion-exchanged sites as isolated Cu^{2+} improved the activity at high temperatures, which suppressed the competitive oxidation of NH_3. Cortés-Reyes et al.[28] synthesized Cu/SAPO-34 catalysts in a one-pot process, and found Cu^{2+} existed in the interior of the cavities. Martínez-Franco et al.[29] obtained Cu/SAPO-34 catalysts by adopting the co-directing SDA, and concluded that it was easy to control the Cu^{2+} loading in the Cu/SAPO-34 catalysts. Tang et al.[30] investigated the effect of Cu^{2+} loading on the SCR activity of Cu/SAPO-34 synthesized by one-pot method.

Generally, ion-exchange method contains several complex steps, which needs long production period and

produces a large amount of wastewater. In contrast, the one-pot method requires a simple hydrothermal synthesis, which is more economical and efficient preparation technology for Cu/SAPO-34. Inspired from previous researches, here, we fabricated metal-incorporated SAPO-34 catalysts by one-step hydrothermal synthesis, investigated the effects of various parameters including the types of metal ions, copper ion sources, SDAs, hydrothermal temperature and time on catalyst activity of metal-incorporated SAPO-34 catalysts, characterized the morphology, structure, and chemical composition of metal-incorporated SAPO-34 catalysts by SEM, XRD, XPS and N_2 adsorption techniques.

2. Experimental

2.1 Fabrication of catalysts

Metal-incorporated SAPO-34 catalysts (Cu/SAPO-34, Fe/SAPO-34 and Mn/SAPO-34) were prepared by a one-pot synthesis method. Figure 1 showed the schematic diagram for the preparation of metal-incorporated SAPO-34 catalysts. In the synthesis procedure, phosphoric acid was firstly dissolved in deionized water, and then silica source (fumed silica) and alumina source (pseudoboehmite) were added into the solution and stirred for 1 h. Subsequently, metals ion sources ($Fe(NO_3)_3 \cdot 9H_2O$, $Mn(CH_3COO)_2 \cdot 4H_2O$ or $Cu(CH_3COO)_2 \cdot H_2O$) and SDAs (tetraethylenepentamine (TEPA)) were introduced to the above gel under continuous stirring for 3 h. The molar composition of

the synthesized gel was: 1Al:0.8P:0.18Si:0.58Metal (Fe, Mn or Cu):0.4SDA (TEPA, TETA or DETA):18H_2O. The resultant gel was sealed in a 100-ml Teflon-lined autoclave, and crystallized in drying oven for 7 days at 150 °C. The obtained products were centrifuged and washed with distilled water, then dried at 100 °C overnight, followed by calcination at 550 °C for 5 h. In order to further optimize the preparation parameters of Cu/SAPO-34 catalysts, various Cu^{2+} sources ($Cu(CH_3COO)_2 \cdot H_2O$, $Cu(NO_3)_3 \cdot 3H_2O$, $CuSO_4 \cdot 5H_2O$ or $CuCl_2 \cdot 2H_2O$,), and SDAs (tetraethylenepentamine (TEPA), Triethylenetetramine (TETA) or Diethylenetriamine (DETA)) were adopted to fabricate Cu/SAPO-34 catalysts at hydrothermal temperature of 100-200 °C for 1-7 days.

2.2 Characterization

The crystal structures of catalysts were analyzed by X-ray diffraction (XRD) via a computer controlled diffractometer (Rigaku D/max-2400) with Cu Kα radiation (λ = 1.54178 Å) at the tube voltage of 40 kV and the current of 100 mA. The pore structure properties of catalysts were investigated by N_2 adsorption-desorption measurements (Quantachrome autosorb-iQ$_2$ Analyzer). The catalysts were degassed at 180 °C for 10 h under vacuum before measurements. The morphology of catalysts were examined by scanning electron microscope (SEM) (Philips XL-30FEG EDX). The elemental composition of catalysts was carried out by X-ray photoelectron spectroscopy (XPS) (Thermo SCIENTIFIC ESCALAB 250 spectrometer). The SCR activity of catalysts
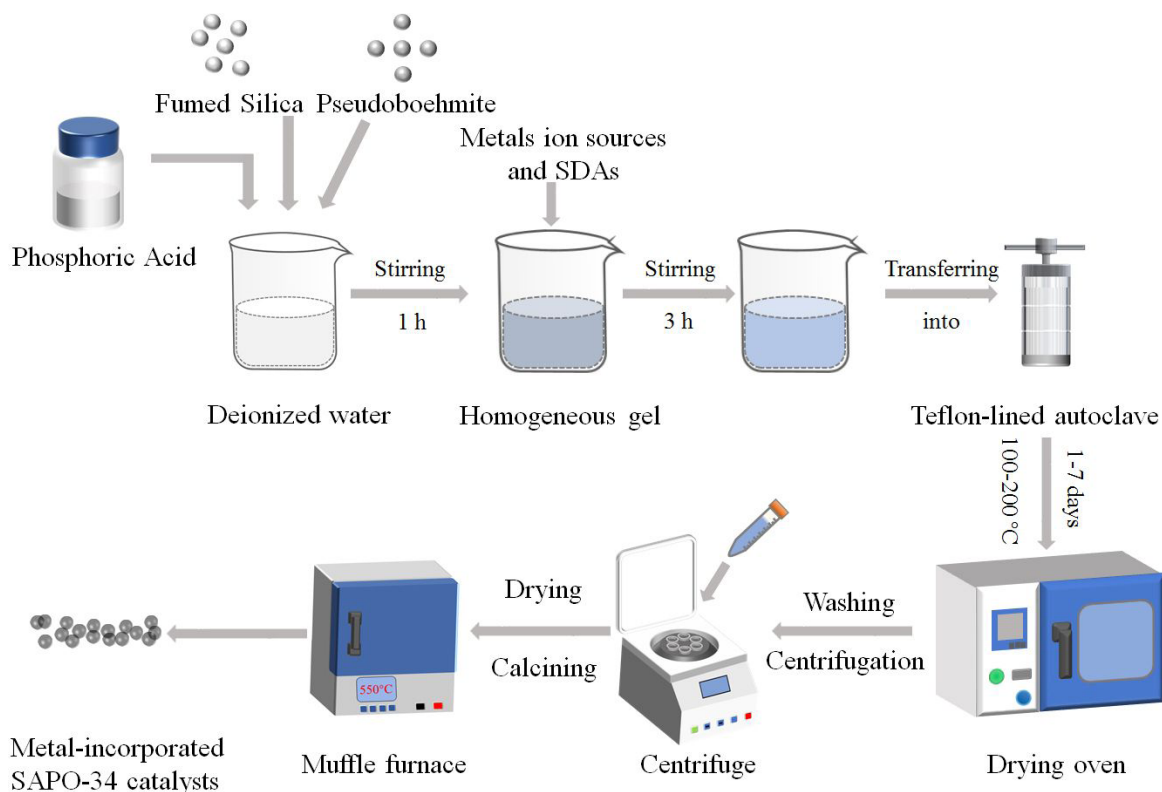

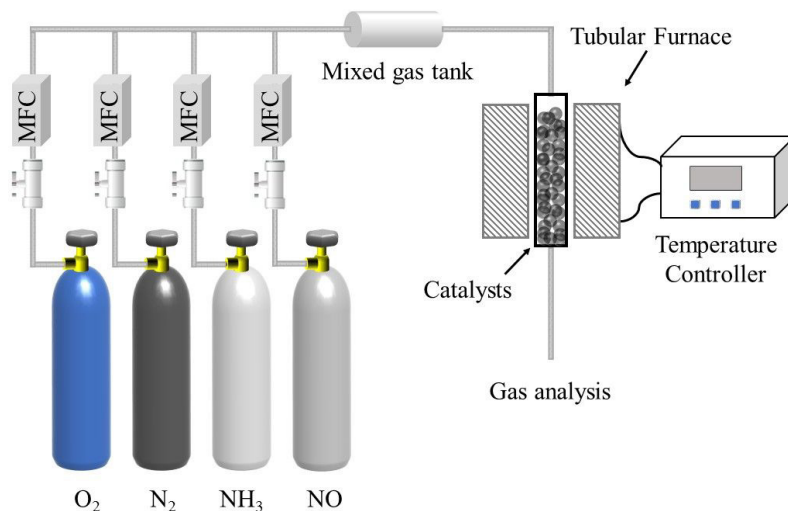**Figure 1.** Flow chart for the preparation of metal-incorporated catalysts.

Figure 2. Schematic diagram for catalytic activity measurement.
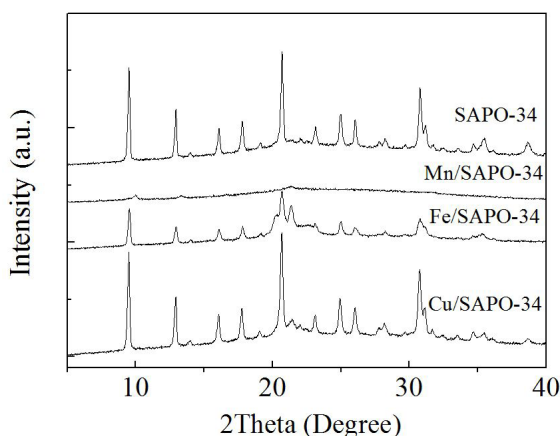

Figure 3. XRD patterns of SAPO-34 catalyst and SAPO-34 catalysts doped with different metal ion sources.

were measured in a fixed-bed quartz reactor. The schematic diagram of catalytic activity measurement was shown in Figure 2, and the detailed test process could refer to our previous paper[31].

3. Results and Discussion

3.1 Effects of incorporated metal ions

For studying the effects of different metal ion sources on the resultant catalytic activity, the SAPO-34 catalysts doped with Cu^{2+}, Fe^{3+} and Mn^{2+} were synthesized at 150 °C for 7 days. Figure 3 demonstrated the XRD patterns of SAPO-34, Cu/SAPO-34, Fe/SAPO-34 and Mn/SAPO-34 catalysts obtained under the same crystallization conditions. Cu/SAPO-34 catalyst possessed characteristic peaks of SAPO-34 at 2θ values 9.5°, 12.7°, 16°, 21°, 25°, and 32° assigned to the chabazite phase, which agreed well with those SAPO-34 (JCPDS: 01-087-1527) in previous paper[32]. The Cu precursor did not induce a significant effect on the crystal structure of the obtained sample. Fe/

SAPO-34 catalyst demonstrated similar characteristics with Cu/SAPO-34 catalyst, but indicated slightly weak peak intensities[33,34]. Subsequently, the degree of crystallinity was calculated by dividing the area of crystalline peaks by the total area under the diffraction curve (crystalline plus amorphous peaks). The degrees of crystallinity for these catalysts were 85.4% for SAPO-34, 80.94% for Fe/SAPO-34, 88.32% for Cu/SAPO-34 respectively, which further supported the above discussion. However, as for Mn/SAPO-34 catalyst, the XRD pattern indicated a predominance of amorphous material. The calculated crystallinity of Mn/SAPO-34 was only 32.58%, which was much lower than that of SAPO-34 (85.4%), implying the destruction of the catalyst structure after the introduction of Mn^{2+} in SAPO-34.

The SEM images shown in Figure 4 presented the morphology of these catalysts. All of the three metal-incorporated SAPO-34 samples were cubic-like catalysts. Cu/SAPO-34 catalyst showed relatively intact microstructure with cubic-like morphology, which were similar with SAPO-34. However, for Fe/SAPO-34 and Mn/SAPO-34 catalysts, they all demonstrated larger size than SAPO-34. We also observed some broken crystal fragments appeared on the surface of Fe/SAPO-34 catalyst and even more broken cubic-like structure existed in Mn/SAPO-34 catalyst, which were responsible for the decrease of crystallinity, agreeing with the XRD analysis. Figure 5 provided the nitric oxide conversion rate of the three catalysts. It displayed that when using Cu and Fe species as active centers, the resultant catalyst indicated high catalytic activity for nitric oxide conversion than SAPO-34 and Mn/SAPO-34 catalyst. The active temperature window of Cu/SAPO-34 catalyst was wider (150-550 °C), while the Fe/SAPO-34 catalyst was slightly narrower (200-450 °C), and the conversion rate of the Cu/SAPO-34 catalyst remained above 80% during 450-600 °C. Based on the above analysis, it was concluded that loading copper ions could greatly improve the crystallinity and active temperature windows compared with other metal ions. Therefore, copper ions were selected as the catalytic active center of SAPO-34.
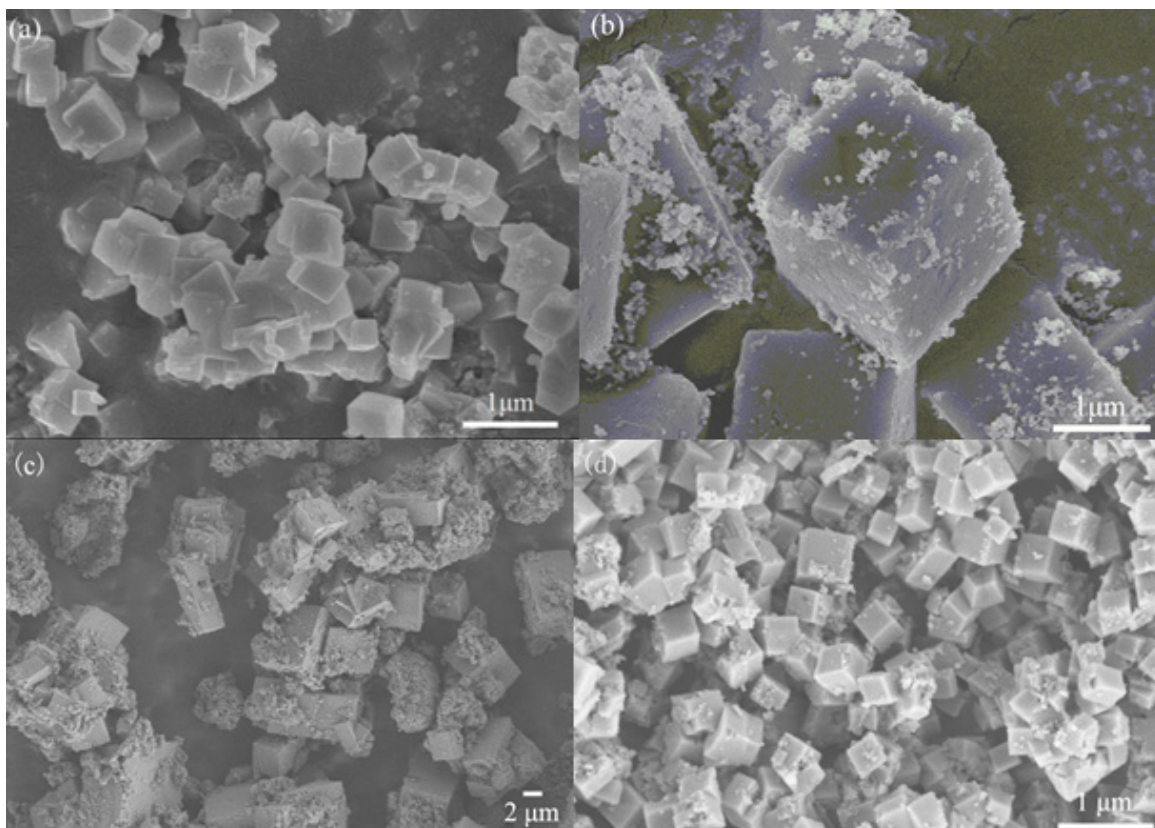
Figure 4. SEM images of various SAPO-34 catalysts: (a) Cu/SAPO-34; (b) Fe/SAPO-34; (c) Mn/SAPO-34; (d) SAPO-34.
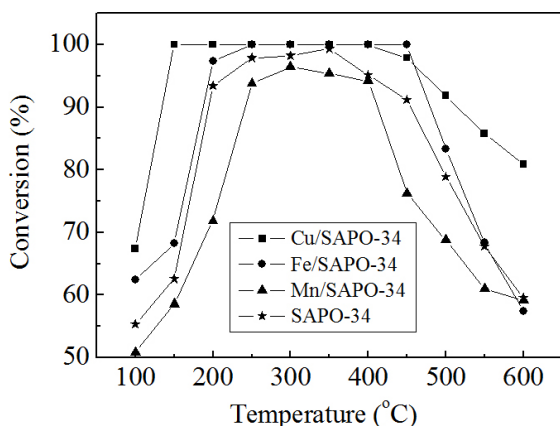

Figure 5. Nitric oxide conversion rate for the SAPO-34 at different metal ion sources.

3.2 Effects of copper ion sources

After defined copper ions were the favorable active site of SAPO-34 catalyst, we further investigated the relationship between different Cu^{2+} sources ($Cu(COOH)_2$, $CuSO_4$, $CuCl_2$, $Cu(NO_3)_2$, and) and SCR performance. It was obvious that the characteristic peaks were observed in all of the four catalysts synthesized at 150 °C for 7 days (Figure 6), which agreed with those reported in the literatures[30,35], and indicated Cu/SAPO-34 catalysts with the four types of Cu^{2+} sources

were all successfully obtained. There were no significant different on diffraction peaks derived from different copper ion sources, which implied that the crystalline structure of the catalysts were almost not affected by the copper ion sources. The degrees of crystallinity for these four catalysts were also very close, which were 88.32%, 87.94%, 86.87%, 87.49% for $Cu(COOH)_2$, $CuSO_4$, $CuCl_2$, $Cu(NO_3)_2$ as Cu^{2+} sources, respectively. SEM images further confirmed the result from XRD analysis. Although different copper ion sources were adopted, the morphologies of these resultant catalysts were similar, and they all showed cubic-like microstructures (Figure 7).

The XPS wide scan spectrum of the Cu/SAPO-34 catalyst was presented in Figure 8a. Al, Si, Cu, P, C, N and O were detected in, displaying the obtained catalyst was SAPO-34 structure containing Cu^{2+}. Figure 8b presented the high resolution spectrum of Cu 2p, which displayed two shake-up satellite peaks at 935.6 and 955.3 eV, corresponding to Cu $2p_{3/2}$ and Cu $2p_{1/2}$, respectively. Generally, these two peaks were used as a characteristic to determine copper ions, implying that copper ions had been successfully loaded in SAPO-34 catalyst and mainly existed as the Cu^{2+} state[36,37].

The result of nitrogen adsorption-desorption isotherms of Cu/SAPO-34 was showed in Figure 9. All catalysts demonstrated typical IV curves with the hysteresis loop. The BET surface area ranged from 232.49-250.29 m^2/g, especially, the largest BET surface area was derived from $Cu(CH_3COO)_2$ with 250.29 m^2/g and performed strong adsorption and desorption capacity.

Figure 10 provided that nitric oxide conversion rates of Cu/SAPO-34 catalysts obtained from four kinds of Cu^{2+} sources. It can observed that the effects of Cu^{2+} sources on the nitric oxide conversion rates of the resultant Cu/SAPO-34 catalysts were not significant. Combined with the above analysis on their morphologies and nitrogen adsorption-desorption characteristics, $Cu(CH_3COO)_2$ was recommended as the candidate Cu^{2+} source for the subsequent experiments.
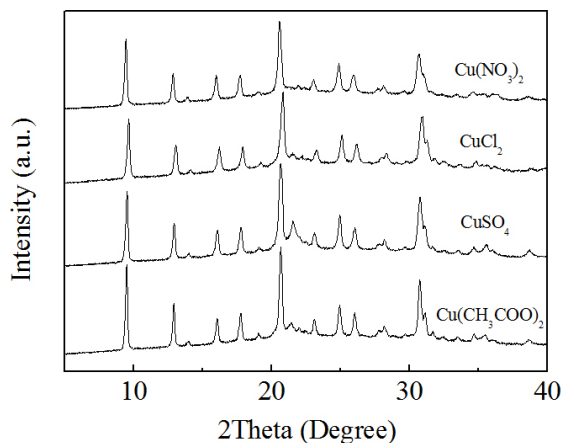

Figure 6. XRD patterns of Cu/SAPO-34 catalysts with different copper ion sources.

3.3 Effects of SDAs

As we known, during the crystallization process, the SDAs play important roles on the physicochemical properties of the synthesized catalysts because of their structure-directing, charge-compensating and space-filling roles[34]. For investigating the effects of SDAs on the performance of catalysts, three SDAs (TEPA, TETA, and DETA) were investigated. XRD patterns of Cu/SAPO-34 catalysts synthesized by the three SDAs at 150 °C for 7 days were showed in Figure 11. Obviously, the Cu/SAPO-34 catalyst synthesized by DETA did not demonstrate the typical characteristic peaks of SAPO-34, which meant that DETA was easy to produce structure defects in the formation of Cu/SAPO-34. However, the Cu/SAPO-34 catalysts adopted TEPA and TETA as SDAs exhibited the chabazite phase of SAPO-34, and the former had a stronger peak intensities, which might be attributed to its good crystal structure. The degrees of crystallinity for the three catalysts were calculated as 88.32%, 83.65%, and 77.16% for TEPA, TETA, and DETA as SDAs, respectively, which agreed with the above analysis.

Figure 12 showed the SEM images of Cu/SAPO-34 catalysts synthesized by the three SDAs. Obviously, the integrity of cubic-like structure of these catalysts was in the order: TEPA>TETA>DETA, and the Cu/SAPO-34 catalyst obtained by using TEPA maintained higher crystal integrity, thus might possess more microspores and active
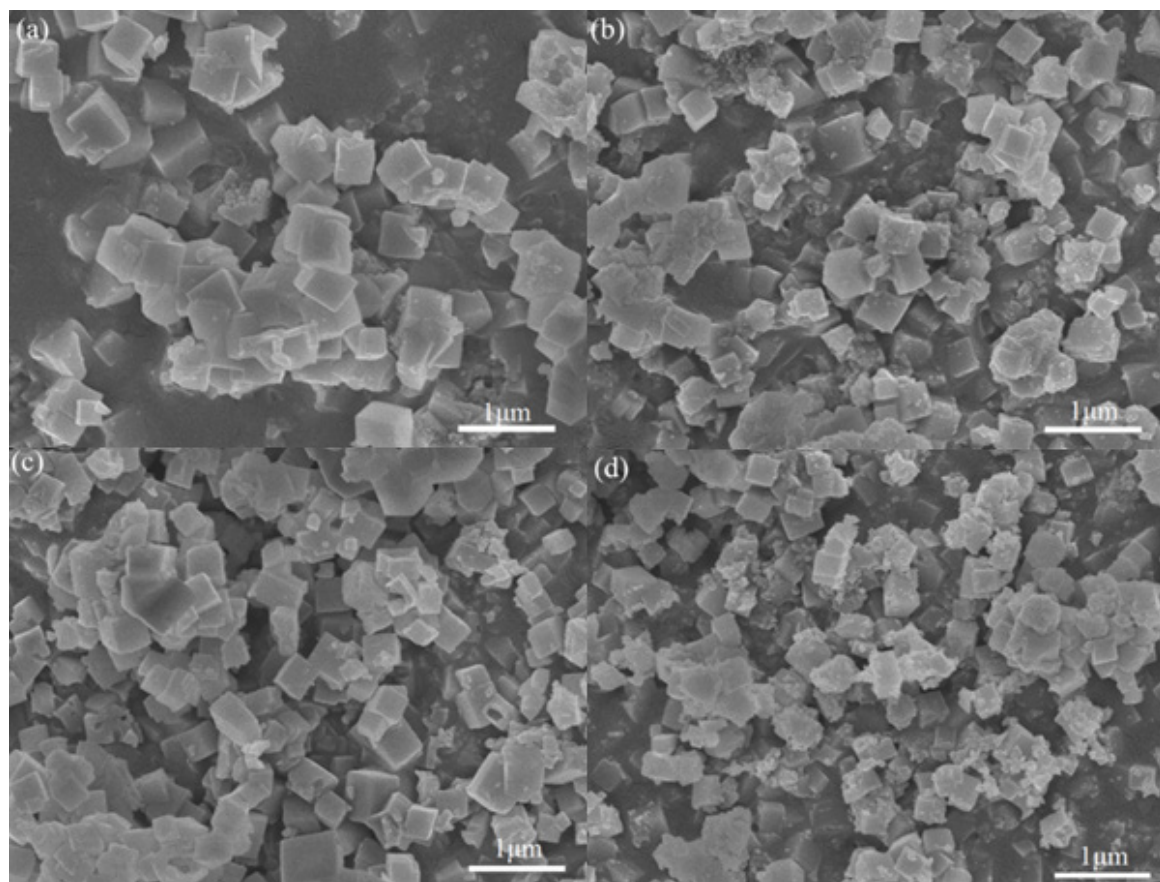

Figure 7. SEM image of Cu/SAPO-34 with different copper ion sources: (a) $Cu(CH_3COO)_2$; (b) $CuSO_4$; (c) $CuCl_2$; (d) $Cu(NO_3)_2$.
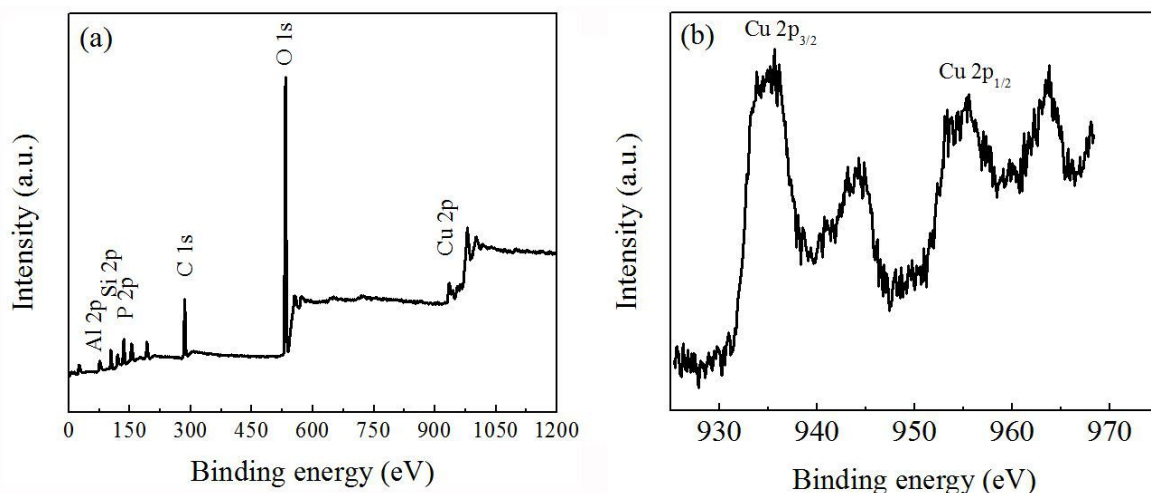
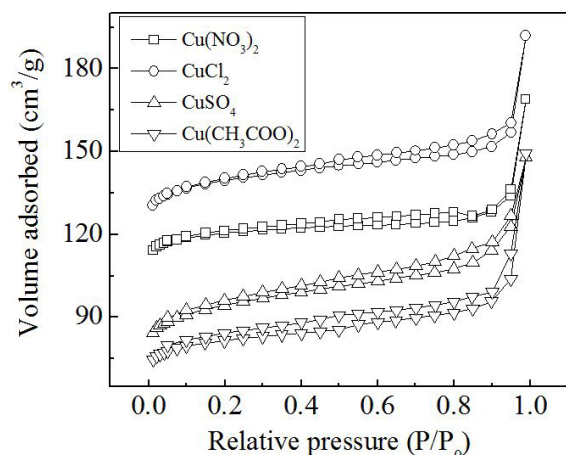**Figure 8.** XPS spectra of Cu/SAPO-34: (a) survey, (b) Cu 2p.

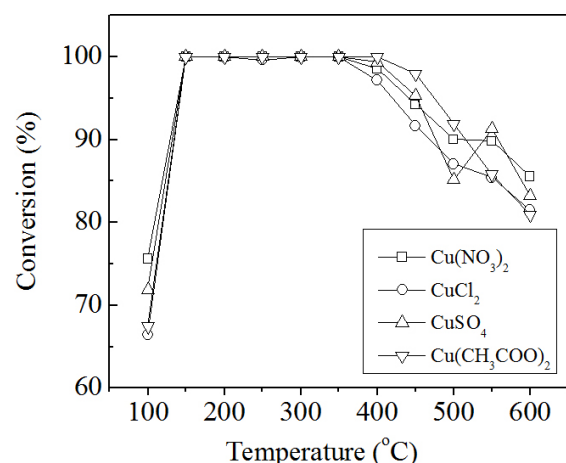**Figure 9.** Nitrogen adsorption-desorption curves of Cu/SAPO-34 catalysts.

Figure 10. Nitric oxide conversion rate for the Cu/SAPO-34 at different copper ions species.

sites, which produced higher SCR catalytic activity[38]. However, as for the Cu/SAPO-34 catalyst prepared from DETA, the incomplete cubic-like structure was observed, which might suppress the diffusion of reactants, declining its catalytic activity.

N_2 adsorption-desorption isotherms were presented in Figure 13. They all demonstrated typical type IV curves, and the corresponding BET surface area of DETA, TETA and TEPA were 40.18 m^2/g, 224.89 m^2/g and 250.29 m^2/g, respectively. The result indicated TEPA had the largest surface areas with strong adsorption and desorption ability for SCR reaction.

Figure 14 presented the nitric oxide conversion rates of the three Cu/SAPO-34 catalysts. When using DETA as SDA, the catalytic activity was extremely unstable throughout the temperature range, and the conversion rate of nitric oxide was significantly low than other two catalysts due to its broken crystal structure. The nitric oxide conversion rates of the Cu/SAPO-34 catalysts obtained by TEPA and TETA as SDAs were rather close with active temperature window range from 150-450 °C. The difference between them was reflected in their catalytic activity above 450 °C, and the reduction of catalytic activity of the former was less than that of the latter.

Sum up, the microstructure and morphology of SAPO-34 varied with the use of different SDAs because SDAs could affect Si coordination structure in SAPO-34[39], which further influenced Cu species distribution in the resultant Cu/SAPO-34 catalyst. Accordingly, the Cu/SAPO-34 catalyst derived from TEPA possessed the largest surface area, demonstrating highest NOx conversion, which agreed with previous results on large specific surface area favored high catalytic activity[40]. Therefore, it was the optimal choice to adopt TEPA as SDA.

3.4 Effects of hydrothermal temperature

For studying the influence of hydrothermal temperature on the structure, morphology, and nitric oxide conversion rate of Cu/SAPO-34 catalysts synthesized at 7 days, XRD

Preparation of Metal-Incorporated SAPO-34 catalysts and their Catalytic Performance in Selective Catalytic Reduction of Nitric Oxide

7

analysis was firstly carried out. The crystallinity of Cu/SAPO-34 was improved as the hydrothermal temperature increased from 100 to 180 °C, and slightly declined at 200 °C (Figure 15). The degrees of crystallinity for these catalysts demonstrated similar trend, which were 30.14%, 39.47%, 88.32%, 88.54%, and 87.62% for the hydrothermal
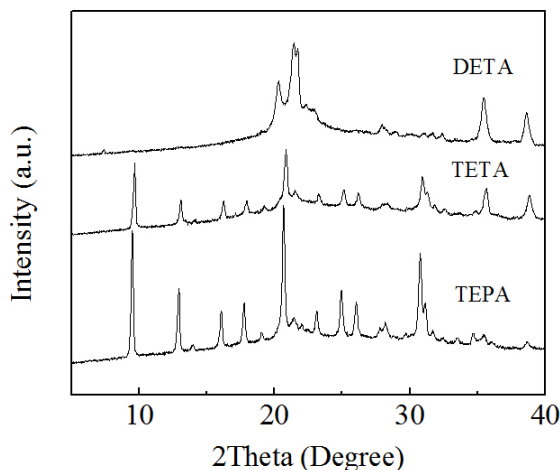

Figure 11. XRD patterns of Cu/SAPO-34 catalysts with different SDAs.

temperature of 100 °C, 120 °C, 150 °C, 180 °C, and 200 °C, respectively. Especially, for the Cu/SAPO-34 samples obtained at 100 and 120 °C, all diffraction peaks did not appear and an amorphous phase was found, which indicated the low hydrothermal temperature could not meet the requirement to synthesize Cu/SAPO-34.

As shown in Figure 16, at low hydrothermal temperature, the synthetic material was irregular fragment crystals, which were basically amorphous substances. The result meant that when the hydrothermal temperature was too low, it was hard to form cubic-like Cu/SAPO-34 catalyst. When increasing the hydrothermal temperature to above 150 °C, the cubic-like Cu/SAPO-34 catalyst started to be formed. The surface of the catalyst was smoother and there was almost no debris crystal attached. Further improved to 200 °C, the crystal size of the catalyst became slight bigger than those catalysts synthesized at other hydrothermal temperatures, which might be attributed to that the crystallization rate of the catalysts were fast at high hydrothermal temperature[41].

Figure 17 showed nitric oxide conversion rate of Cu/SAPO-34 catalysts obtained at various hydrothermal temperatures. Obviously, when the temperature reached 150 °C, the active temperature window was 150-550 °C, and the removal rate of nitric oxide almost reached 100% at 150-450 °C. Therefore, the hydrothermal temperature of 150 °C was recommended for nitric oxide removal in this work.
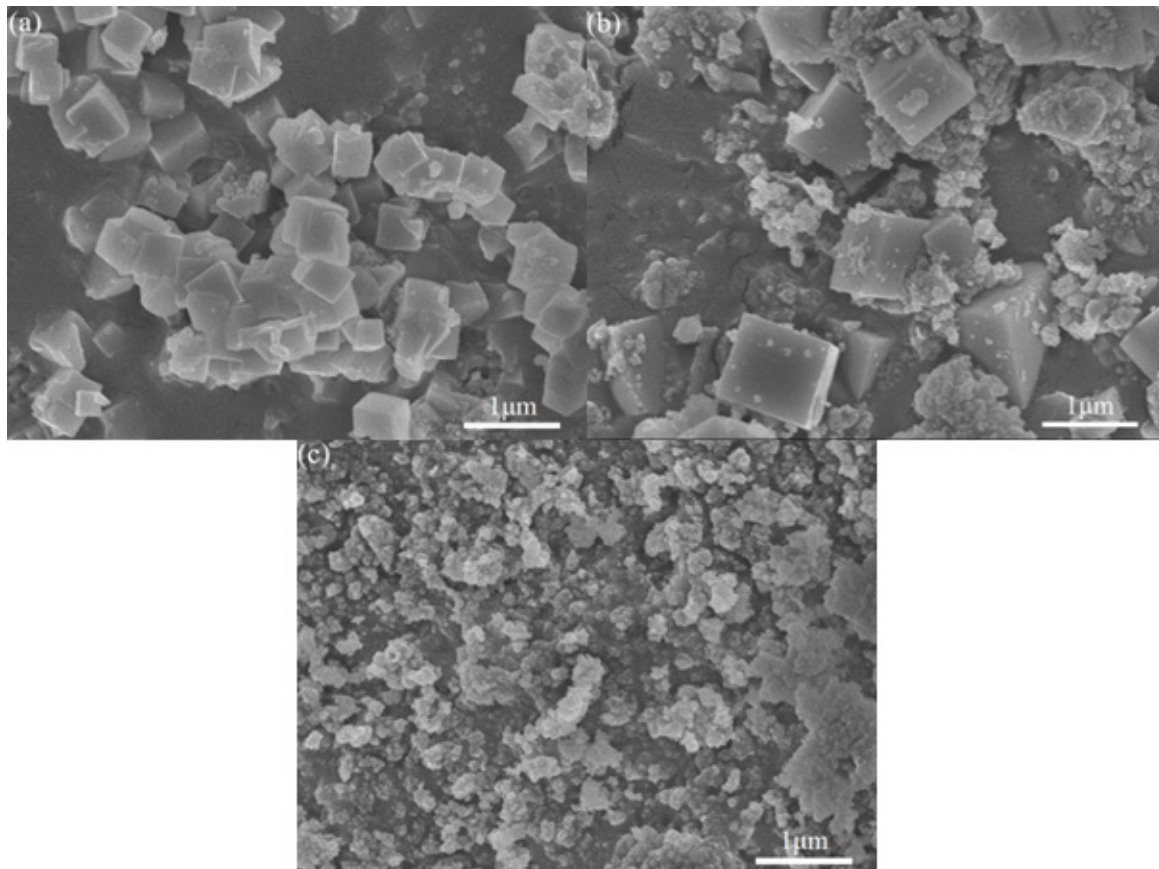

Figure 12. SEM images of Cu/SAPO-34 with different SDAs: (a) TEPA; (b) TETA; (c) DETA.

3. 5 Effects of hydrothermal time

The influences of hydrothermal time on the structure, morphology, and removal efficiency of nitric oxide of Cu/SAPO-34 catalyst synthesized at 150 °C were further
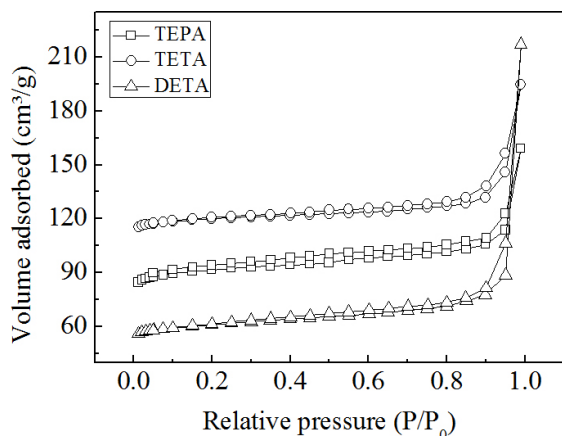

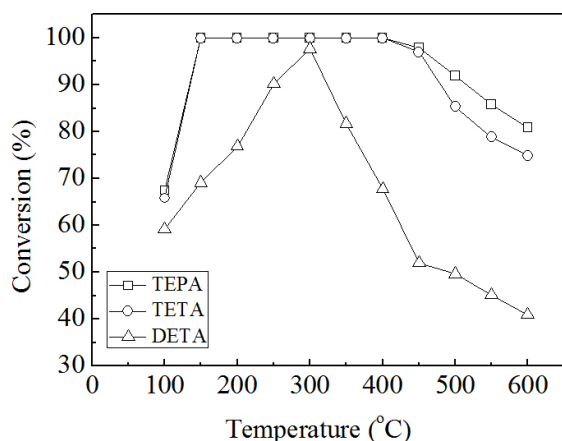**Figure 13.** N$_2$ adsorption-desorption isotherms of Cu/SAPO-34 catalysts.

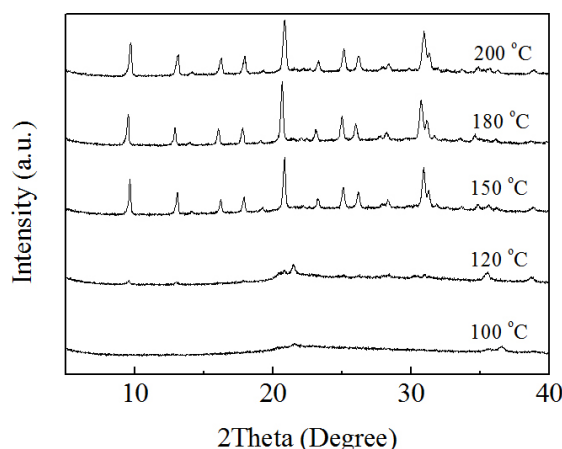**Figure 14.** Nitric oxide conversion rates for the Cu/SAPO-34 at different SDAs.

Figure 15. XRD patterns of Cu/SAPO-34 catalysts with various hydrothermal temperatures.

evaluated. Obviously, short hydrothermal time (1 day) led to the produce of Cu/SAPO-34 catalyst with poor crystallinity (Figure 18), which was calculated as 79.06%. Improving the hydrothermal time to 3 days, the stronger peak intensities were indicated, suggesting the formation Cu/SAPO-34 catalyst with good crystallinity (85.77%). Extending the hydrothermal time to 7 days, the peak intensities were further increased, the degrees of crystallinity was improved to 88.32%. The SEM images provided by Figure 19 also approved the conclusion from XRD analysis. At 1 day of hydrothermal time, incomplete cubic-like structure was observed. When the hydrothermal reaction exceeded 3 days, the synthesized Cu/SAPO-34 catalysts revealed relatively complete cubic-like morphology.

Figure 20 presented the nitric oxide conversion rates of Cu/SAPO-34 catalysts synthesized at the hydrothermal time of 1, 3, and 7 days, respectively. Obviously, the nitric oxide conversion rates of the three Cu/SAPO-34 catalysts were improved dramatically with the increase of reaction temperature below 150 °C, and then stayed stable. As the reaction temperature exceeded 350 °C, the nitric oxide conversion rate began to decline for the Cu/SAPO-34 catalyst synthesized at short hydrothermal time (1 day). However, for the two Cu/SAPO-34 catalysts synthesized at 3 and 7 days, almost the same trends on nitric oxide conversion rates were observed before 500 °C, however, slight high nitric oxide conversion rates were observed due to its good crystallinity at long hydrothermal time.

Four kinds of reported Cu/SAPO-34 catalysts (ion-exchange method and one-pot method) were used for comparison with our catalysts. Wang et al.[26] reported the ion-exchanged Cu/SAPO-34 catalyst, which demonstrated low catalyst activity (about 20% -70% of nitric oxide conversion rate) below 350 °C, and even at the high reaction temperature range of 350-550 °C, the nitric oxide conversion rates only remained at about 70-80%. Liu et al.[27] presented their work on ion-exchanged Cu/SAPO-34 catalyst, and the catalyst indicated high catalyst activity (above 80% of nitric oxide conversion rate) at reaction temperature range of 200-350 °C. As for "one-pot" synthesized Cu/SAPAO-34 catalysts, they usually demonstrated higher catalyst activity than those obtained by ion-exchange method. For example, Martínez-Franco et al.[29] fabricated high activity Cu/SAPAO-34 catalyst via one-pot method. The resultant catalyst showed excellent catalyst activity (above 80% of nitric oxide conversion rate) at the whole reaction temperature range (200-500 °C), and especially at 250-400 °C, nitric oxide conversion rate reached 100%. Tang et al.[30] got high activity Cu/SAPAO-34 catalyst via one-pot method, and nitric oxide conversion rates were above 80% at reaction temperature of 200-600 °C. In this work, we also obtained the Cu/SAPAO-34 catalyst by one-pot hydrothermal method, its catalyst activity was close to that obtained by Martínez-Franco et al.[29] by one-pot method, and higher than those fabricated by Tang et al.[30] via one-pot method, and Wang et al.[26] and Liu et al.[27] via ion-exchange method.
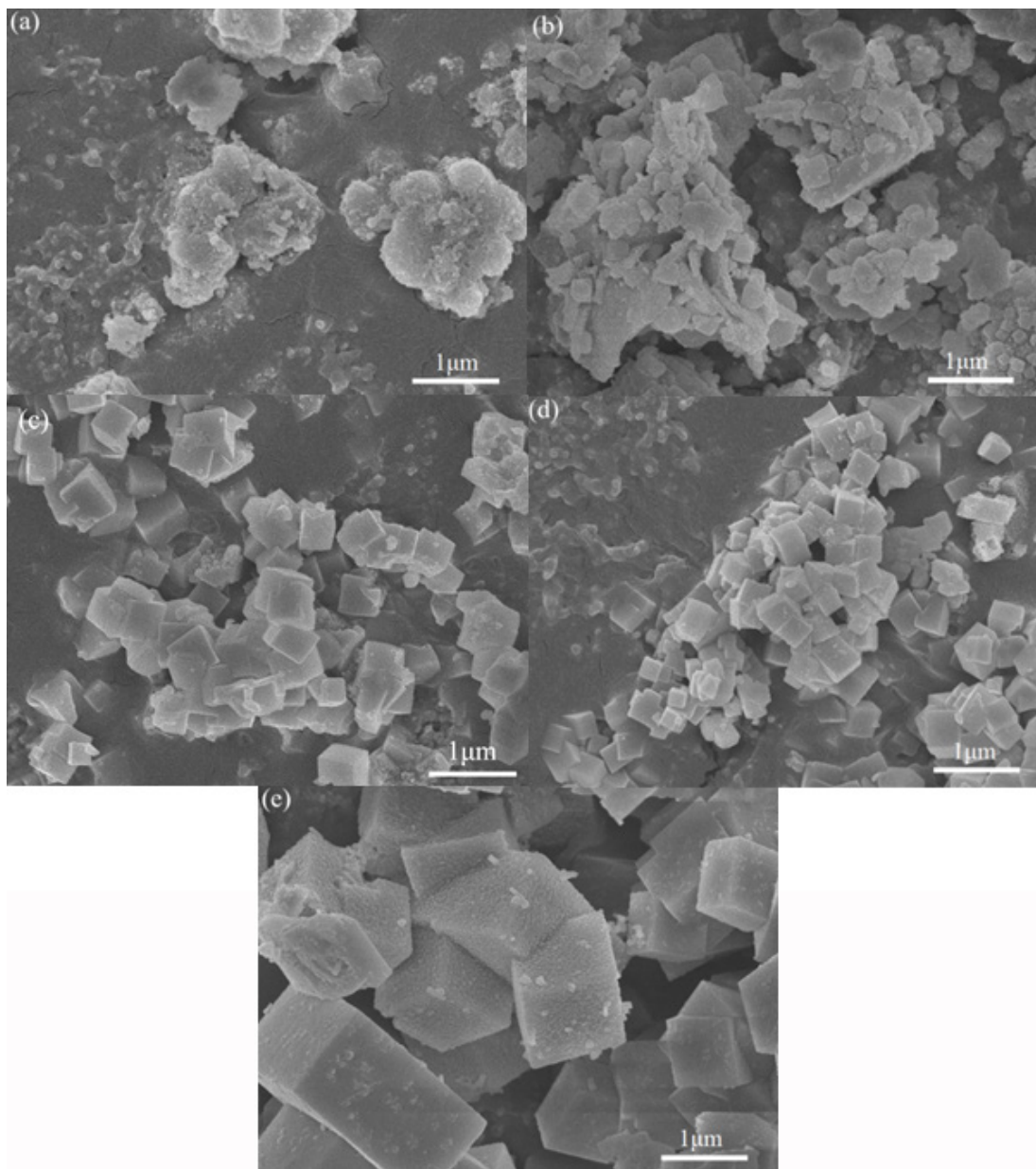
Figure 16. SEM images of Cu/SAPO-34 catalyst:(a) 100 °C;(b) 120 °C;(c) 150 °C;(d) 180 °C;(e) 200 °C.
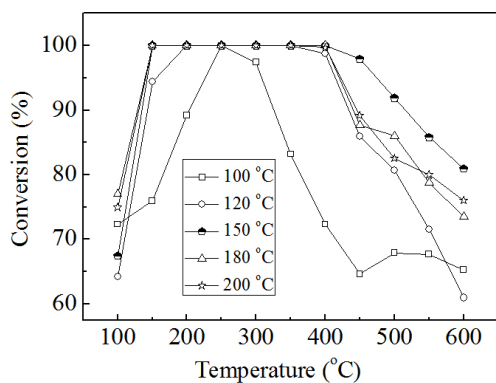

Figure 17. Nitric oxide conversion rate for the Cu/SAPO-34 at different hydrothermal temperatures.
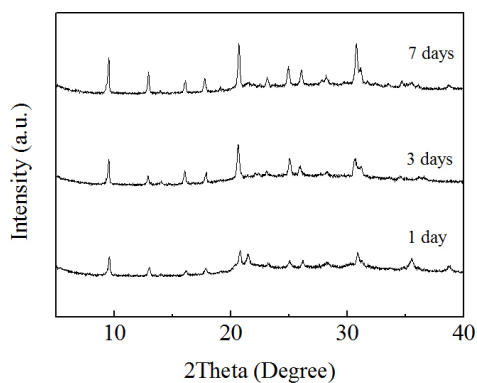

Figure 18. XRD patterns of Cu/SAPO-34 catalysts at different hydrothermal time.
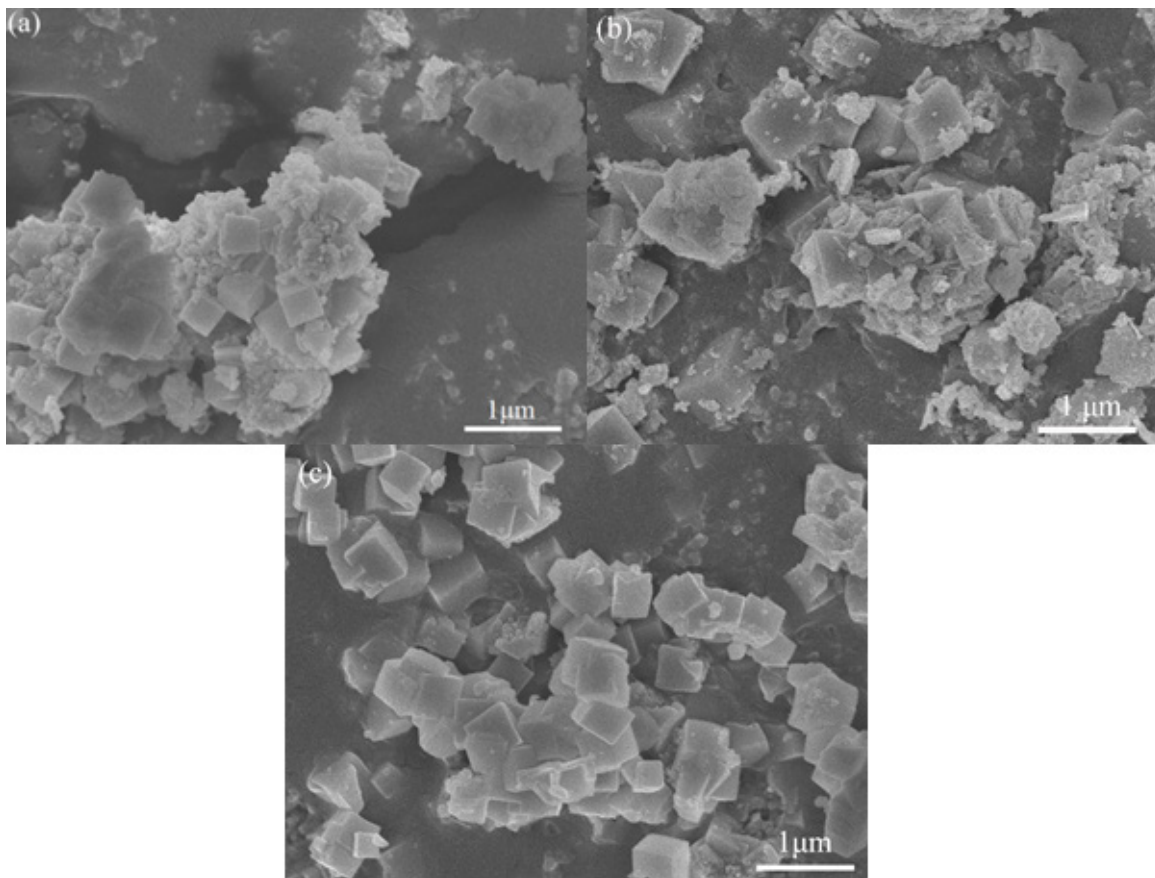
Figure 19. SEM images of Cu/SAPO-34 catalyst at different hydrothermal time: (a) 1 day; (b) 3 days; (c) 7 days.
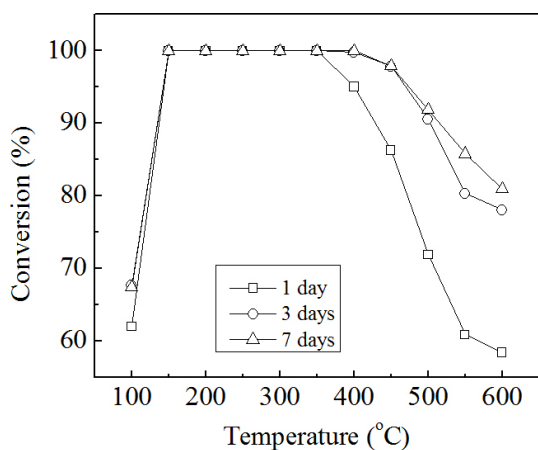

Figure 20. Nitric oxide conversion rates for the Cu/SAPO-34 at different hydrothermal time.

4. Conclusion

In summary, we have successfully fabricated various metal-incorporated SAPO-34 catalysts via one-step hydrothermal synthesis. Among them, Cu/SAPO-34 catalysts demonstrated complete microstructure with cubic morphology, wide temperature window, and high nitric oxide conversion rate. Subsequently, A series of Cu/SAPO-34 catalysts were synthesized using four kinds of copper salts ($CuSO_4$, $Cu(NO_3)_2$, $CuCl_2$, and $Cu(COOH)_2$) as Cu^{2+} sources, and found that Cu^{2+} sources did not produce significant influence on the nitric oxide conversion rates of the resultant Cu/SAPO-34 catalyst. SDAs had an important impact on properties of the synthesized Cu/SAPO-34 catalysts, and the Cu/SAPO-34 catalyst adopting TEPA as SDA could maintain higher crystal integrity and active sites, which were benefit to the SCR reaction. Furthermore, hydrothermal temperature and time had significant influences on the formation of Cu/SAPO-34 catalyst. When the hydrothermal temperature was higher than 150 °C and the hydrothermal time was longer than 3 days, the Cu/SAPO-34 catalyst with a cubic-like structure and high catalyst activity could be obtained.

6. References

1. Huang X, Zhang S, Chen H, Zhong Q. Selective catalytic reduction of NO with NH_3 over V_2O_5 supported on TiO_2 and Al_2O_3: a comparative study. J Mol Struct. 2015;1098:289-97.
2. Skalska K, Miller JS, Ledakowicz S. Trends in NOx abatement: a review. Sci Total Environ. 2010;408:3976-89.

Preparation of Metal-Incorporated SAPO-34 catalysts and their Catalytic Performance in Selective Catalytic
Reduction of Nitric Oxide

11

3. Kompio PGWA, Brückner A, Hipler F, Auer G, Löffler E, Grünert W. A new view on the relations between tungsten and vanadium in V_2O_5-WO_3/TiO_2 catalysts for the selective reduction of NO with NH_3. J Catal. 2012;286:237-47.

4. Yang J, Sun R, Sun S, Zhao N, Hao N, Chen H, et al. Experimental study on NOx reduction from staging combustion of high volatile pulverized coals. Part 1. Air staging. Fuel Process Technol. 2014;126:266-75.

5. Ma Z, Wu X, Si Z, Weng D, Ma J, Xu T. Impacts of niobia loading on active sites and surface acidity in NbOx/CeO_2–ZrO_2 NH_3–SCR catalysts. Appl Catal B. 2015;179:380-94.

6. Koebel M, Elsener M, Kleemann M. Urea-SCR: a promising technique to reduce NOx emissions from automotive diesel engines. Catal Today. 2000;59:335-45.

7. Ma Z, Yang H, Liu F, Zhang X. Interaction between SO_2 and Fe–Cu–Ox/CNTs–TiO_2 catalyst and its influence on NO reduction with NH_3. Applied Catalysis A. 2013;467:450-5.

8. Song Z, Zhang Q, Ning P, Fan J, Duan Y, Liu X, et al. Effect of CeO_2 support on the selective catalytic reduction of NO with NH_3 over P-W/CeO_2. J Taiwan Inst Chem Engrs. 2016;65:149-61.

9. Mees FDP, Martens LRM, Janssen MJG, Verberckmoes AA. Vansant EFImprovement of the hydrothermal stability of SAPO-34. Chem Commun. 2003;1:44-5.

10. Briend M, Vomscheid R, Peltre MJ, Man PP, Barthomeuf D. Influence of the choice of the template on the short- and long-term stability of SAPO-34 zeolite. J Chem Phys. 1995;99:8270-6.

11. Wang D, Tian P, Yang M, Xu S, Fan D, Su X, et al. Synthesis of SAPO-34 with alkanolamines as novel templates and their application for CO_2 separation. Microporous Mesoporous Mater. 2014;194:8-14.

12. Gao F, Wang Y, Kollár M, Washton NM, Szanyi J, Peden CHF. A comparative kinetics study between Cu/SSZ-13 and Fe/SSZ-13 SCR catalysts. Catal Today. 2015;258:347-58.

13. Martínez-Franco R, Moliner M, Thogersen JR, Corma A. Efficient one-pot preparation of Cu-SSZ-13 materials using cooperative OSDAs for their catalytic application in the SCR of NOx. ChemCatChem. 2013;5:3316-23.

14. Gao F, Kollár M, Kukkadapu RK, Washton NM, Wang Y, Szanyi J, et al. Fe/SSZ-13 as an NH_3-SCR catalyst: a reaction kinetics and FTIR/Mössbauer spectroscopic study. Appl Catal B. 2015;164:407-19.

15. Wen C, Geng L, Han L, Wang J, Chang L, Feng G, et al. A comparative first principles study on trivalent ion incorporated SSZ-13 zeolites. Phys Chem Chem Phys. 2015;17:29586-96.

16. Carja G, Kameshima Y, Okada K, Madhusoodana CD. Mn–Ce/ZSM5 as a new superior catalyst for NO reduction with NH_3. Appl Catal B. 2007;73:60-4.

17. Liu Z, Yi Y, Zhang S, Zhu T, Zhu J, Wang J. Selective catalytic reduction of NOx with NH_3 over Mn-Ce mixed oxide catalyst at low temperatures. Catal Today. 2013;216:76-81.

18. Cao F, Su S, Xiang J, Wang P, Hu S, Sun L, et al. The activity and mechanism study of Fe–Mn–Ce/γ-Al_2O_3 catalyst for low temperature selective catalytic reduction of NO with NH_3. Fuel. 2015;139:232-9.

19. Wang J, Fan D, Yu T, Wang J, Teng H, Hu X, et al. Improvement of low-temperature hydrothermal stability of Cu/SAPO-34 catalysts by Cu^{2+} species. J Catal. 2015;322:84-90.

20. Fickel DW, D'Addio E, Lauterbach JA, Lobo RF. The ammonia selective catalytic reduction activity of copper-exchanged small-pore zeolites. Appl Catal B. 2011;102:441-8.

21. Ma L, Cheng Y, Cavataio G, McCabe RW, Fu L, Li J. Characterization of commercial Cu-SSZ-13 and Cu-SAPO-34 catalysts with hydrothermal treatment for NH_3-SCR of NOx in diesel exhaust. Chem Eng J. 2013;225:323-30.

22. Fan S, Xue J, Yu T, Fan D, Hao T, Shen M, et al. The effect of synthesis methods on Cu species and active sites over Cu/SAPO-34 for NH_3-SCR reaction. Catal Sci Technol. 2013;3:2357-64.

23. Liu Z, Tang L, Chang L, Wang J, Bao W. In situ synthesis of Cu-SAPO-34/cordierite for the catalytic removal of NOx from diesel vehicles by C_3H_8. Chin J Catal. 2011;32:546-54.

24. Martínez-Franco R, Moliner M, Concepcion P, Thogersen JR, Corma A. Synthesis, characterization and reactivity of high hydrothermally stable Cu-SAPO-34 materials prepared by "one-pot" processes. J Catal. 2014;314:73-82.

25. Wang J, Yu T, Wang X, Qi G, Xue J, Shen M, et al. The influence of silicon on the catalytic properties of Cu/SAPO-34 for NOx reduction by ammonia-SCR. Appl Catal B. 2012;127:137-47.

26. Wang L, Li W, Qi G, Weng D. Location and nature of Cu species in Cu/SAPO-34 for selective catalytic reduction of NO with NH_3. J Catal. 2012;289:21-9.

27. Liu X, Wu X, Weng D, Si Z, Ran R. Evolution of copper species on Cu/SAPO-34 SCR catalysts upon hydrothermal aging. Catal Today. 2017;281:596-604.

28. Cortés-Reyes M, Finocchio E, Herrera C, Larrubia MA, Alemany LJ, Busca G. A study of Cu-SAPO-34 catalysts for SCR of NOx by ammonia. Microporous Mesoporous Mater. 2016;241:258-65.

29. Martínez-Franco R, Moliner M, Franch C, Kustov A, Corma A. Rational direct synthesis methodology of very active and hydrothermally stable Cu-SAPO-34 molecular sieves for the SCR of NOx. Appl Catal B. 2012;127:273-80.

30. Tang J, Xu M, Yu T, Ma H, Shen M, Wang J. Catalytic deactivation mechanism research over Cu/SAPO-34 catalysts for NH_3–SCR (II): the impact of copper loading. Chem Eng Sci. 2017;168:414-22.

31. Tao P, Sun MH, Qu SC, Song CW, Li C, Yin YY, et al. Effects of V_2O_5 and WO_3 loadings on the catalytic performance of V_2O_5-WO_3/TiO_2 catalyst for SCR of NO with NH_3. Glob NEST J. 2017;19(1):160-6.

32. Mirza K, Ghadiri M, Haghighi M, Afghan A. Hydrothermal synthesize of modified Fe, Ag and K-SAPO-34 nanostructured catalysts used in methanol conversion to light olefins. Microporous Mesoporous Mater. 2018;260:155-65.

33. Wei Y, Zhang D, Xu L, Chang F, He Y, Meng S, et al. Synthesis, characterization and catalytic performance of metal-incorporated SAPO-34 for chloromethane transformation to light olefins. Catal Today. 2008;131:262-9.

34. Sena FC, de Souza BF, de Almeida NC, Cardoso JS, Fernandes LD. Influence of framework composition over SAPO-34 and MeAPSO-34 acidity. Applied Catalysis A. 2011;406:59-62.

35. Wang J, Peng Z, Chen Y, Bao W, Chang L, Feng G. In-situ hydrothermal synthesis of Cu–SSZ-13/cordierite for the catalytic removal of NOx from diesel vehicles by NH_3. Chem Eng J. 2015;263:9-19.

36. Wang J, Chen Y, Tang L, Bao W, Chang L, Han L. One-step hydrothermal synthesis of Cu–SAPO-34/cordierite and its catalytic performance on NOx removal from diesel vehicles. Trans Nonferrous Met Soc China. 2013;23:3330-6.

37. Liu J, Yu F, Liu J, Cui L, Zhao Z, Wei Y, et al. Synthesis and kinetics investigation of meso-microporous Cu-SAPO-34 catalysts for the selective catalytic reduction of NO with ammonia. J Environ Sci. 2016;48:45-58.

38. Feng X, Lin Q, Cao Y, Zhang H, Li Y, Xu H, et al. Neodymium promotion on the low-temperature hydrothermal stability of a Cu/SAPO-34 NH_3-SCR monolith catalyst. J Taiwan Inst Chem Engrs. 2017;80:805-12.

39. Pastore HO, Coluccia S, Marchese L. Porous Aluminophosphates: from molecular sieves to designed acid catalysts. Annu Rev Mater Res. 2005;35:351-95.

40. Li J, Song Z, Ning P, Zhang Q, Liu X, Li H, et al. Influence of calcination temperature on selective catalytic reduction of NOx with NH_3 over CeO_2-ZrO_2-WO_3 catalyst. J Rare Earths. 2015;33:726-35.

41. Wang X, Li R, Bakhtiar SH, Yuan F, Li Z, Zhu Y. Excellent catalytic performance for methanol to olefins over SAPO-34 synthesized by controlling hydrothermal temperature. Catal Commun. 2018;108:64-7.